

# A BACKWARD KOLMOGOROV EQUATION APPROACH TO COMPUTE MEANS, MOMENTS AND CORRELATIONS OF NON-SMOOTH STOCHASTIC DYNAMICAL SYSTEMS

Laurent Mertz<sup>\*</sup>, Georg Stadler<sup>†</sup>, and Jonathan Wylie<sup>‡</sup>

**ABSTRACT.** We present a computational alternative to probabilistic simulations for non-smooth stochastic dynamical systems that are prevalent in engineering mechanics. As examples, we target (1) stochastic elasto-plasticity, which involve transitions between elastic and plastic states, and (2) obstacle problems with noise, which involve discrete impulses due to collisions with an obstacle. We focus on solving Backward Kolmogorov Equations (BKEs) of stochastic variational inequalities modelling elasto-plastic and obstacle oscillators. The main challenge in solving BKEs corresponding to these problems is to deal with the non-standard boundary conditions which describe the behavior of the underlying process on the boundary. Applications that could make use of this framework abound in many areas of science and technology.

## 1. MOTIVATIONS AND GOAL

In this paper, we propose a computational alternative to probabilistic simulations for a certain type of non-smooth stochastic dynamical systems, namely

$$(1) \quad \dot{X}_t = F(X_t, Y_t), \quad \dot{Y}_t = G(X_t, Y_t) + \mathbf{H}_t + \dot{W}_t, \quad \forall t > 0$$

with initial condition  $(X_0, Y_0) = (x, y) \in \mathbb{R}^2$ . Here,  $(X_t, Y_t) \in \mathbb{R}^2$  is the state variable at time  $t$ , dots denote derivatives with respect to time,  $F(x, y)$  and  $G(x, y)$  are deterministic functions,  $\dot{W}$  represents a white noise random forcing in the sense that  $W$  is a Wiener process, and  $\mathbf{H}$  is a functional depending on interactions of the state variable at boundaries and interfaces. We are interested in statistical quantities that characterize and help predicting the behavior of  $\{(X_t, Y_t), t \geq 0\}$  such as means, moments and correlations. They are of the form

$$A \triangleq \mathbb{E} \left( f(X_T, Y_T) + \int_0^T g(X_\tau, Y_\tau) d\tau \right), \quad B \triangleq \mathbb{E} \left( \int_0^\infty e^{-\lambda\tau} g(X_\tau, Y_\tau) d\tau \right),$$

$$C \triangleq \lim_{T \rightarrow \infty} \mathbb{E} (f(X_T, Y_T))$$

---

<sup>\*</sup>ECNU-NYU Institute of Mathematical Sciences, NYU Shanghai, Shanghai, China

<sup>†</sup>Courant Institute of Mathematical Sciences, New York University, New York, USA

<sup>‡</sup>Department of Mathematics, City University of Hong Kong, Hong Kong, China

and

$$\begin{aligned} A' &\triangleq \mathbb{E} \left[ \left( f(X_T, Y_T) + \int_0^T g(X_\tau, Y_\tau) d\tau \right) \left( \varphi(X_{T+h}, Y_{T+h}) + \int_0^{T+h} \psi(X_\tau, Y_\tau) d\tau \right) \right], \\ B' &\triangleq \mathbb{E} \left( \int_0^\infty \int_0^\infty e^{-\lambda\tau - \mu\theta} g(X_\tau, Y_\tau) \psi(X_\theta, Y_\theta) d\tau d\theta \right), \\ C' &\triangleq \lim_{T \rightarrow \infty} \frac{1}{T} \mathbb{E} \left( \int_0^T \int_0^T g(X_\tau, Y_\tau) \psi(X_\theta, Y_\theta) d\tau d\theta \right). \end{aligned}$$

Here and in the remainder of the paper,  $\mu, \lambda$  are positive numbers,  $T > 0$  is a given time,  $h \geq 0$  and  $f, g, \varphi, \psi$  are continuous functions. For cases in which  $\mathbf{H} \equiv 0$  and  $(F, G)$  satisfy appropriate smoothness conditions, a natural setting for characterizing such quantities is to use Backward Kolmogorov Equations (BKEs) [20]. Furthermore, if in addition  $F$  and  $G$  can be written in terms of a Hamiltonian structure  $\mathcal{H}(x, y)$ , in the sense

$$F(x, y) \triangleq \frac{\partial \mathcal{H}}{\partial x}(x, y), \quad G(x, y) \triangleq \frac{\partial \mathcal{H}}{\partial y}(x, y) + \eta(x, y) \frac{\partial \mathcal{H}}{\partial x}(x, y), \quad (x, y) \in \mathbb{R}^2,$$

where  $\eta$  is a well behaved function, then the process  $(X_t, Y_t)$  belongs to the class of Stochastic Hamiltonian Systems (SHS) [21] for which quantities of type  $C$  and  $C'$  are well defined. Applications that make use of this framework abound in many areas of science and engineering, e.g., finance, chemistry, biology, neuroscience, economy and mechanics.

There are many important applications involving non-smooth dynamics in which quantities of the form  $A, B, C$  and  $A', B', C'$  are of interest. We have in mind problems involving interactions with boundaries, constraints, phase transitions or hysteresis. An important class of examples includes elasto-plasticity (EP) problems with random forcing [12, 15] where the dynamics takes into account phase transitions between elastic and plastic states. A second class of examples includes stochastically driven obstacle problems [1, 11] where the dynamics has to take into account instantaneous collisions with an obstacle.

From a mathematical viewpoint, these problems can be reformulated in terms of (degenerate) stochastic variational inequalities [2, 8]. With this formulation, the evolution of the state variables is Markovian and Kolmogorov Equations (KEs) can be derived.

Except for very few non-smooth dynamical systems, where analytical expressions are available, in general one has to resort to computational techniques to determine  $A, B, C$  and  $A', B', C'$ . The most straightforward computational methods are direct probabilistic simulations. Such techniques are simple to implement and widely used. For low-dimensional state variables, they are less efficient than techniques based on partial differential equations (PDEs), provided the latter are available. For the two non-smooth stochastic processes targeted in this paper, the presence of constraints or phase transitions (governed by a variational inequality structure) leads to non-standard boundary conditions in the BKEs. These boundary conditions characterize the behavior of the underlying process on the boundary. This paper is concerned with the numerical treatment of such non-standard KEs and their application to compute the quantities of  $A, B, C$  and  $A', B', C'$ .

We point out that the idea of solving non-standard BKEs in the context of a SVI has been used before [3]. However, the technique in [3] is specific to the elasto-perfectly-plastic oscillator excited by white noise, for which the non-standard condition has to be satisfied in a finite (namely two) number of points. It has no natural extension to problems of obstacle type because for these problems the non-standard condition must be satisfied on a continuous set of points.

In the remainder of this section, we give the definitions of the elasto-plastic and obstacle models in presence of noise, and we discuss the quantities we are interested in.

**1.1. Elasto-plastic problem with noise.** A basic prototype for modeling mechanical structures that admit permanent deformation under vibrations is the elastic-plastic oscillator [15]. The dynamics focuses on two quantities: the total deformation,  $X_t$ , supported by the structure when subjected to vibrations, and its velocity,  $\dot{X}_t$ . For general elasto-plastic problems, the nonlinear functional  $\mathbf{H}$  in (1) is a restoring force arising from the structure. The exact form of  $\mathbf{H}$  depends on the particular structure in question. The nonlinearity in such models comes from the switching of regimes from an elastic phase to a plastic one, or vice versa. For the elasto-perfectly-plastic oscillator (EPPO) model, the irreversible (plastic) deformation  $\Delta$  and the reversible (elastic) deformation  $Z$  at time  $t$  satisfy

$$\begin{aligned} \dot{Z}_t &= \dot{X}_t, & \dot{\Delta}_t &= 0, & \text{in elastic phase,} \\ \dot{\Delta}_t &= \dot{X}_t, & \dot{Z}_t &= 0, & \text{in plastic phase,} \end{aligned}$$

where  $X_t = Z_t + \Delta_t$ . Typically,  $|Z_t|$  is bounded by a given threshold  $P_Y$  at all times  $t$ , the system is in the plastic phase when  $|Z_t| = P_Y$  and the elastic phase when  $|Z_t| < P_Y$ . Here,  $P_Y$  is an elasto-plastic bound, known as the “Plastic Yield” in the engineering literature. We assume the force  $\mathbf{H}$  is a linear function of  $Z$  (while  $\Delta$  remains constant) in the elastic phase and a constant (while  $Z$  remains constant at  $\pm P_Y$ ) in the plastic phase as follows:

$$(2) \quad \mathbf{H}_t = kZ_t, \quad k > 0.$$

The permanent (plastic) deformation at time  $t$  can then be written as

$$\Delta_t = \int_0^t \mathbf{1}_{\{|Z_s| = P_Y\}} Y_s ds.$$

We will also consider the case of linearly damped spring for which  $F(x, y) = y$  and  $G(x, y) = -c_0 y$ .

*SVI framework.* It has been shown that the dynamics of such a nonlinear oscillator can be described mathematically by means of SVIs [8]. The dynamics is then described by the pair  $(Y_t, Z_t)$  that satisfies

$$(3) \quad dY_t = -(c_0 Y_t + kZ_t)dt + dW_t, \quad (dZ_t - Y_t dt)(\phi - Z_t) \geq 0, \quad \forall |\phi| \leq P_Y, \forall t,$$

and appropriate initial conditions for  $Y_0$  and  $Z_0$  must be prescribed. Here, whereas  $Y_t = \dot{X}_t$ ,  $X_t$  is not involved in the dynamics.

Characterizing the statistics of the state variable through its KE is important for engineering purposes. To illustrate the robustness and efficiency of our approach we will compute four important quantities in this paper:

- the probability of finding the system in the plastic state

$$(E_1) \quad \mathbb{P}(|Z_T| = P_Y) \text{ for } T \geq 0, \quad \text{and} \quad \lim_{T \rightarrow \infty} \mathbb{P}(|Z_T| = P_Y),$$

- the mean kinetic energy

$$(E_2) \quad \mathbb{E}Y_T^2 \text{ for } T \geq 0, \quad \text{and} \quad \lim_{T \rightarrow \infty} \mathbb{E}Y_T^2,$$

- the variance of both the plastic deformation and the total deformation

$$(E_3) \quad \sigma^2(\Delta_T), \quad \sigma^2(X_T) \text{ for } T \geq 0, \quad \text{and} \quad \lim_{T \rightarrow \infty} \frac{1}{T} \sigma^2(\Delta_T), \quad \lim_{T \rightarrow \infty} \frac{1}{T} \sigma^2(X_T),$$

- any correlation structure between  $(Y_T, Z_T)$  and  $(Y_{T+h}, Z_{T+h})$  of the form

$$\mathbb{E}f(X_T, Y_T)\varphi(X_{T+h}, Y_{T+h}),$$

where here we will target

$$(E_4) \quad \mathbb{P}(|Z_{T+h}| = P_Y, |Z_T| = P_Y), \quad \mathbb{E}Y_T^2 Y_{T+h}^2 \text{ for } T \geq 0,$$

and

$$\lim_{T \rightarrow \infty} \mathbb{P}(|Z_{T+h}| = P_Y, |Z_T| = P_Y), \quad \lim_{T \rightarrow \infty} \mathbb{E}Y_T^2 Y_{T+h}^2.$$

The probability of finding the system in the plastic state and the mean kinetic energy, at a given time  $T$ , are quantities of type  $A$  whereas, at large time, they are of type  $C$ . Also, their Laplace transforms belong to type  $B$ . The variance of the plastic deformation and of the total deformation, at a given time  $T$ , are quantities of type  $A'$  and their asymptotic growth belongs to the type  $C'$ . Any correlation structure of  $(Y, Z)$  between two different instants  $T$  and  $T + h$  is of type  $A'$  and its corresponding double Laplace transform (with parameters  $\lambda$  and  $\mu$ ) is of type  $B'$ . These quantities are challenging to compute because analytic formulas are not available and probabilistic simulations are computationally expensive.

**1.2. Obstacle problem with noise.** One of the simplest models exhibiting a vibro-impact motion can be expressed as a single degree of freedom oscillator constrained by obstacles [1] located at  $|X| = P_O$  (position of the obstacle). It is common in the engineering literature to formulate the dynamics of a stochastic obstacle oscillator in terms of a stochastic process  $X_t$ , the oscillator displacement. For general obstacle problems, the nonlinearity in such models comes from the collisions. If at a time  $t$ , the state hits the obstacle with incoming velocity  $\dot{X}_t$ , it immediately bounces back with velocity  $-e\dot{X}_t$ , that is,  $\dot{X}_{t+} = -e\dot{X}_{t-}$ ,  $e \in [0, 1]$ . The nonlinear functional  $\mathbf{H}$  in (1) is a force keeping track of the past discrete impulses due to collisions with an obstacle, here

$$(4) \quad \mathbf{H}_t = \dot{I}_t.$$

The net impulse process, which keeps track of the sum of all past impulses, at time  $t$  can be written as

$$I_t \triangleq \sum_{\{0 \leq s \leq t: |X_s| = P_O\}} \dot{X}_{s+} - \dot{X}_{s-}.$$

For simplicity, we consider the case of a linearly damped spring:  $F(x, y) = y$  and  $G(x, y) = -c_0 y - kx$ .

*SVI framework.* From a mathematical viewpoint (using a stochastic differential framework), the dynamics of such a nonlinear oscillator can be described in the framework of SVIs [2] as follows

$$(5) \quad (dY_t + (c_0 Y_t + kX_t)dt - dW_t)(\varphi - X_t) \geq 0, \quad \forall |\varphi| \leq P_O, |X_t| \leq P_O, \forall t,$$

where  $Y_t \triangleq \dot{X}_t$ . This must be supplemented by the impact rule  $Y_{t+} = -eY_{t-}$ .

For the obstacle problem, we consider the following four quantities:

- the probability of finding the system in the neighborhood of the obstacle with a low velocity,

$$(E'_1) \quad \mathbb{P}(f(X_T, Y_T) \leq \epsilon), \text{ for } T \geq 0, \quad \text{and} \quad \lim_{T \rightarrow \infty} \mathbb{P}(f(X_T, Y_T) \leq \epsilon) \text{ for some } \epsilon > 0$$

where  $f(x, y) \triangleq \sqrt{(|x| - 1)^2 + y^2}$ .

- the mean kinetic energy

$$(E'_2) \quad \mathbb{E}Y_T^2 \text{ for } T \geq 0, \quad \text{and} \quad \lim_{T \rightarrow \infty} \mathbb{E}Y_T^2,$$

- the variance of the integral of the displacement

$$(E'_3) \quad \sigma^2 \left( \int_0^T X_s ds \right) \text{ for } T \geq 0, \quad \text{and} \quad \lim_{T \rightarrow \infty} \frac{1}{T} \sigma^2 \left( \int_0^T X_s ds \right).$$

Up to a multiplicative constant, this is equivalent to computing the variance of the change in momentum due to the restoring force  $kX$ .

- any correlation structure between  $(X_T, Y_T)$  and  $(X_{T+h}, Y_{T+h})$  of the form

$$(E'_4) \quad \mathbb{P}(f(X_{T+h}, Y_{T+h}) \leq \epsilon, f(X_T, Y_T) \leq \epsilon), \quad \mathbb{E}Y_T^2 Y_{T+h}^2 \text{ for } T \geq 0,$$

and

$$\lim_{T \rightarrow \infty} \mathbb{P}(f(X_{T+h}, Y_{T+h}) \leq \epsilon, f(X_T, Y_T) \leq \epsilon), \quad \lim_{T \rightarrow \infty} \mathbb{E}Y_T^2 Y_{T+h}^2.$$

An explanation similar to what was provided above for the elasto-plastic problem (in terms of plastic state, variance of the plastic deformation and correlations) applies to the obstacle problem (in terms of mean kinetic energy, variance of the integral of the displacement and correlations).

**1.3. Approach and overview.** The PDEs related to  $A, B, C$  and  $A', B', C'$  including quantities  $(E_i)$ ,  $(E'_i)$ ,  $1 \leq i \leq 4$  for the elasto-plastic and obstacle problems are non-standard boundary value problems. For this type of non-standard PDEs, (for instance see Theorem 6, Theorem 7 in Section 2.2), only partial existence and uniqueness results are available, mainly for the case of the EPPO problem with noise [4, 7–9]. This is because standard PDE theory techniques do not apply due to the non-standard boundary conditions and the degeneracy of these problems. Therefore, in this essay, we mostly study the behavior of these PDEs numerically in order to gather insight in the solution behavior and we compare with probabilistic approximations in order to conjecture whether solutions exist or not. For this purpose, we solve the PDE problems on sequences of grids with increasing resolution and monitor the behavior of the numerical solutions. If the numerical solutions computed from differently accurate discretization yield a converging behavior as the mesh is refined, we can conjecture that the continuous problem has a solution.

Monte Carlo methods are used to compare the PDE results with probabilistic results. These comparisons increase our confidence in the solution of the PDE problem, allow us to study approximation errors in both schemes, and establish a direct connection between the SVIs and the PDE problems.

**1.4. Organization of the paper.** In section 2, we show the connection between the quantities  $A$  and  $A'$  to the solution of non-standard *parabolic problems*, the functions  $B$  and  $B'$  to the solution of non-standard *elliptic problems* and the functions  $C$  and  $C'$  to the solution of non-standard *Poisson problems*. In Section 3, we present a numerical approach for solving non-standard BKEs. The method is first presented and applied to the elasto-plastic problem. Then, it is applied to the obstacle problem. Numerical results are presented. In Section 4, we compare the approach proposed in this paper with previous techniques employed for a white noise EPPO. Finally, in Section 5, broader impacts of the present method are discussed for promising engineering applications.

## 2. THE PARTIAL DIFFERENTIAL EQUATIONS FOR $A, B, C$ AND $A', B', C'$

It is possible to relate the functions  $A$  and  $A'$  to the solution of *parabolic problems*, the functions  $B$  and  $B'$  to the solution of *elliptic problems* and the functions  $C$  and  $C'$  to the solution of *Poisson problems*. In the first part of this section, we present these problems in the case of  $\mathbf{H} = 0$ . Then, in the second part, we provide a formal presentation of the corresponding problems for the two non-smooth problems targeted in this paper.

For  $T > 0$  and a domain  $\Omega$  of  $\mathbb{R}^2$ , we use the notation  $C^*(\Omega \times [0, T])$  for the set of continuous functions on  $\Omega \times [0, T]$  that are  $C^1$ -regular with respect to  $x$ ,  $C^2$ -regular with respect to  $y$  and  $C^1$ -regular with respect to  $t$ . We use the notation  $C^*(\Omega)$  for the set of continuous functions on  $\Omega$  that are  $C^1$ -regular with respect to  $x$  and  $C^2$ -regular with respect to  $y$ . We use the generic notation  $\Gamma$  for

$$\Gamma_T^\lambda(f, g) \triangleq e^{-\lambda T} f(X_T, Y_T) + \int_0^T e^{-\lambda \tau} g(X_\tau, Y_\tau) d\tau$$

because it helps to write the quantities  $A, B, C$  and  $A', B', C'$  in a compact form.

**2.1. The case  $\mathbf{H} = 0$ .** Here, Proposition 1 connects the solution of (1) to PDEs related to  $A, B, C$  and  $A', B', C'$ .

**Proposition 1.** *For any function  $\phi \in C^*(\mathbb{R}^2 \times [0, \infty])$  satisfying*

$$(A_\lambda^\phi) \quad \mathbb{E} \left( \int_0^t e^{-2\lambda \tau} \left| \frac{\partial \phi}{\partial y} \right|^2 (X_\tau, Y_\tau, \tau) d\tau \right) < \infty, \forall t$$

*the process*

$$(6) \quad M_t^{\lambda, \phi} \triangleq e^{-\lambda t} \phi(X_t, Y_t, t) - \int_0^t e^{-\lambda \tau} \left( \frac{\partial \phi}{\partial t} + L\phi - \lambda \phi \right) (X_\tau, Y_\tau, \tau) d\tau$$

*satisfies*

$$(7) \quad M_t^{\lambda, \phi} = \phi(x, y, 0) + \int_0^t e^{-\lambda \tau} \frac{\partial \phi}{\partial y} (X_\tau, Y_\tau, \tau) dW_\tau$$

where  $L$  is the differential operator

$$L \triangleq \frac{1}{2} \frac{\partial^2}{\partial y^2} + F \frac{\partial}{\partial x} + G \frac{\partial}{\partial y}.$$

Thus  $M_t^{\lambda, \phi}$  is a martingale under  $\mathcal{F}_t \triangleq \sigma\{W_s, 0 \leq s \leq t\}$ . Moreover, for any function  $\phi' \in C^*(\mathbb{R}^2 \times [0, \infty])$  satisfying  $(\mathcal{A}_\mu^{\phi'})$  (8)

$$\mathbb{E} \left( M_T^{\lambda, \phi} M_{T+h}^{\mu, \phi'} \right) = \phi \phi'(x, y, 0) + \mathbb{E} \left( \int_0^T e^{-(\lambda+\mu)\tau} \frac{\partial \phi}{\partial y} \frac{\partial \phi'}{\partial y} (X_\tau, Y_\tau, \tau) d\tau \right), \quad \forall T \geq 0, \quad \forall h \geq 0.$$

*Proof.* From the assumption on  $\phi$  the stochastic integral  $\int_0^t e^{-\lambda\tau} \frac{\partial \phi}{\partial y} (X_\tau, Y_\tau, \tau) dW_\tau$  is well defined. Thus, (7) is obtained by using Ito's formula,

$$e^{-\lambda t} \phi(X_t, Y_t, t) - \phi(x, y, 0) = \int_0^t e^{-\lambda\tau} \left( \frac{\partial \phi}{\partial t} + L\phi - \lambda\phi \right) (X_\tau, Y_\tau, \tau) d\tau + \int_0^t e^{-\lambda\tau} \frac{\partial \phi}{\partial y} (X_\tau, Y_\tau, \tau) dW_\tau.$$

Therefore  $M_t^{\lambda, \phi}$  is a martingale with respect to  $\mathcal{F}_t$ . Similarly for  $\phi'$ ,

$$M_t^{\mu, \phi'} = \phi'(x, y, 0) + \int_0^t e^{-\mu\tau} \frac{\partial \phi'}{\partial y} (X_\tau, Y_\tau, \tau) dW_\tau.$$

Hence, (8) is obtained using Ito's isometry.  $\square$

**Theorem 2** (Backward-in-time parabolic problems). *Consider functions  $u \in C^*(\mathbb{R}^2 \times [0, T])$ ,  $v \in C^*(\mathbb{R}^2 \times [0, T+h])$ ,  $w \in C^*(\mathbb{R}^2 \times [0, T])$ . Assume that  $u, v, w$  satisfy  $(\mathcal{A}_\lambda^u)$ ,  $(\mathcal{A}_\mu^v)$ ,  $(\mathcal{A}_{\lambda+\mu}^w)$ , respectively, and that*

$$(9) \quad \frac{\partial u}{\partial t} + Lu - \lambda u = -g, \quad u(T) = f \quad \text{in } \mathbb{R}^2, \quad \frac{\partial v}{\partial t} + Lv - \mu v = -\psi, \quad v(T+h) = \varphi \quad \text{in } \mathbb{R}^2, \\ \text{and}$$

$$(10) \quad \frac{\partial w}{\partial t} + Lw - (\lambda + \mu)w = -\frac{\partial u}{\partial y} \frac{\partial v}{\partial y}, \quad w(T) = 0 \quad \text{in } \mathbb{R}^2.$$

Then we have

$$A = u(x, y, 0) \quad \text{and} \quad A' = (uv + w)(x, y, 0).$$

*Proof.* Applying (6)-(7) of Proposition 1 to  $\phi = u$ , the solution of (9), we get

$$\mathbb{E} \left( \Gamma_T^\lambda(f, g) \right) = u(x, y, 0).$$

Applying (8) of Proposition 1 to  $\phi = u$  and  $\phi = v$ , we get

$$\mathbb{E} \left( \Gamma_T^\lambda(f, g) \Gamma_{T+h}^\mu(\varphi, \psi) \right) = uv(x, y, 0) + \mathbb{E} \left( \int_0^T e^{-(\lambda+\mu)\tau} \frac{\partial u}{\partial y} \frac{\partial v}{\partial y} (X_\tau, Y_\tau, \tau) d\tau \right).$$

Finally, applying (6)-(7) of Proposition 1 to  $\phi = w$ , the solution of (10), we get

$$w(x, y, 0) = \mathbb{E} \left( \int_0^T e^{-(\lambda+\mu)\tau} \frac{\partial u}{\partial y} \frac{\partial v}{\partial y} (X_\tau, Y_\tau, \tau) d\tau \right).$$

Therefore,

$$\mathbb{E} \left( \Gamma_T^\lambda(f, g) \Gamma_{T+h}^\mu(\varphi, \psi) \right) = (uv + w)(x, y, 0).$$

$\square$

**Corollary 3.** *Under the hypothesis of Theorem 2,*

$$\text{Var}(\Gamma_T^0(f, g)) = w(x, y, 0),$$

where  $w$  solves the problem (10) with  $v = u$  and  $h = 0$ .

*Proof.* This is a direct consequence of Theorem 2.  $\square$

**Theorem 4** (Degenerate elliptic problems). *Consider functions  $u_\lambda, v_\mu, w_{\lambda+\mu} \in C^*(\mathbb{R}^2)$ . Assume that  $u_\lambda, v_\mu, w_{\lambda+\mu}$  satisfy*

$$(\mathcal{A}_1) \quad \left\{ \begin{array}{l} \lim_{T \rightarrow 0} \exp(-\lambda T) \mathbb{E} u_\lambda(X_T, Y_T) = 0, \quad \lim_{T \rightarrow 0} \exp(-\mu T) \mathbb{E} v_\mu(X_T, Y_T) = 0, \\ \lim_{T \rightarrow 0} \exp(-(\lambda + \mu)T) \mathbb{E} w_{\lambda+\mu}(X_T, Y_T) = 0, \\ \int_0^\infty \exp(-\lambda \tau) \mathbb{E} g(X_\tau, Y_\tau) d\tau < \infty, \quad \int_0^\infty \exp(-\mu \tau) \mathbb{E} \psi(X_\tau, Y_\tau) d\tau < \infty, \\ \int_0^\infty \exp(-(\lambda + \mu)\tau) \mathbb{E} \frac{\partial v_\mu}{\partial y} \frac{\partial u_\lambda}{\partial y}(X_\tau, Y_\tau) d\tau < \infty, \end{array} \right.$$

and

$$(\mathcal{A}_2) \quad \left\{ \begin{array}{l} \lim_{T \rightarrow 0} \exp(-(\lambda + \mu)T) \mathbb{E} (u_\lambda v_\mu(X_T, Y_T)) = 0, \\ \lim_{T \rightarrow 0} \exp(-\lambda T) \mathbb{E} \left( u_\lambda(X_T, Y_T) \int_0^T \exp(-\mu \tau) \psi(X_\tau, Y_\tau) d\tau \right) = 0, \\ \lim_{T \rightarrow 0} \exp(-\mu T) \mathbb{E} \left( v_\mu(X_T, Y_T) \int_0^T \exp(-\lambda \tau) g(X_\tau, Y_\tau) d\tau \right) = 0, \end{array} \right.$$

and

$$(11) \quad \left\{ \begin{array}{l} Lu_\lambda - \lambda u_\lambda = -g \quad \text{in } \mathbb{R}^2, \\ Lv_\mu - \mu v_\mu = -\psi \quad \text{in } \mathbb{R}^2, \\ Lw_{\mu+\lambda} - (\mu + \lambda)w_{\lambda+\mu} = -\frac{\partial u_\lambda}{\partial y} \frac{\partial v_\mu}{\partial y} \quad \text{in } \mathbb{R}^2. \end{array} \right.$$

Then we have

$$B = u_\lambda(x, y) \quad \text{and} \quad B' = (u_\lambda v_\mu + w_{\lambda+\mu})(x, y).$$

*Proof.* Under Assumption  $(\mathcal{A}_1)$ , using Proposition 1,

$$\begin{aligned} u_\lambda(x, y) &= \mathbb{E} \int_0^\infty \exp(-\lambda t) g(X_t, Y_t) dt, \quad v_\mu(x, y) = \mathbb{E} \int_0^\infty \exp(-\mu t) \psi(X_t, Y_t) dt \\ w_{\lambda+\mu}(x, y) &= \mathbb{E} \int_0^\infty \exp(-(\lambda + \mu)t) \frac{\partial u_\lambda}{\partial y}(X_t, Y_t) \frac{\partial v_\mu}{\partial y}(X_t, Y_t) dt \end{aligned}$$

and under Assumption  $(\mathcal{A}_2)$ , direct calculations yields

$$\begin{aligned} &\mathbb{E} \int_0^\infty \exp(-(\lambda + \mu)t) \left( \frac{\partial u_\lambda}{\partial y} \frac{\partial v_\mu}{\partial y} \right) (X_t, Y_t) dt + \mathbb{E} \int_0^\infty \exp(-\lambda t) g(X_t, Y_t) dt \mathbb{E} \int_0^\infty \exp(-\mu t) \psi(X_t, Y_t) dt \\ &= \mathbb{E} \int_0^\infty \int_0^\infty \exp(-\lambda s_1) \exp(-\mu s_2) g(X_{s_1}, Y_{s_1}) \psi(X_{s_2}, Y_{s_2}) ds_1 ds_2. \end{aligned}$$

$\square$

Assume that  $(X_t, Y_t)$  has a unique invariant probability measure  $\nu$  on  $\mathbb{R}^2$  in the sense that for any continuous function  $f$  satisfying  $\nu(|f|) < \infty$ , we have  $\mathbb{E}f(X_t, Y_t) = \nu(f)$  provided that  $(X_0, Y_0)$  is distributed according to  $\nu$ . The proof of the following Theorem is similar to the above proofs.

**Theorem 5** (Degenerate Poisson problems). *Consider functions  $U, V \in C^*(\mathbb{R}^2)$ . Assume that  $g$  and  $\psi$  satisfy  $\nu(|g|) < \infty, \nu(|\psi|) < \infty$  and  $U, V$  satisfy*

$$(A_3) \quad \nu \left( \left| \frac{\partial U}{\partial y} \frac{\partial V}{\partial y} \right| \right) < \infty$$

together with

$$(12) \quad LU = \nu(g) - g \quad \text{in } \mathbb{R}^2, \quad LV = \nu(\psi) - \psi \quad \text{in } \mathbb{R}^2.$$

Then we have

$$C = \nu(g) \quad \text{and} \quad C' = \nu \left( \frac{\partial U}{\partial y} \frac{\partial V}{\partial y} \right).$$

**2.2. Non-standard PDEs of SVIs: elasto-plastic and obstacle problems.** In a similar manner to the results above for the case  $\mathbf{H} = 0$ , here we present non-standard PDEs related to SVIs modeling the elasto-plastic (2) and obstacle (4) problems. First, for each problem, we give a description of the infinitesimal generator of the corresponding process for which an analogue of Proposition 1 can be obtained. Then, we only present the non-standard backward-in-time parabolic problems in analogy to Theorem 2. For the non-standard elliptic degenerate and Poisson problems, the idea remains basically the same as in Theorem 4 and Theorem 5.

Without loss of generality, we can assume here that  $P_Y = P_O = 1$ , define

$$D \triangleq (-1, 1) \times (-\infty, \infty), \quad D_T \triangleq (-1, 1) \times (-\infty, \infty) \times (0, T)$$

and

$$D_{\pm} \triangleq \{\pm 1\} \times (-\infty, \infty), \quad D_T^{\pm} \triangleq \{\pm 1\} \times (-\infty, \infty) \times (0, T).$$

In the elasto-plastic problem, using Ito's lemma, the generator of  $(Z_t, Y_t)$  is defined on any function  $\phi \in C^*(\bar{D})$  and satisfies

$$\lim_{t \rightarrow 0} \frac{\mathbb{E}\phi(Z_t, Y_t) - \phi(z, y)}{t} = \begin{cases} L\phi \triangleq \frac{1}{2} \frac{\partial^2 \phi}{\partial y^2} - (c_0 y + kz) \frac{\partial \phi}{\partial y} + y \frac{\partial \phi}{\partial z}, & \text{if } |z| < 1, \\ L_+ \phi \triangleq \frac{1}{2} \frac{\partial^2 \phi}{\partial y^2} - (c_0 y + k) \frac{\partial \phi}{\partial y} + \min(0, y) \frac{\partial \phi}{\partial z}, & \text{if } z = 1, \\ L_- \phi \triangleq \frac{1}{2} \frac{\partial^2 \phi}{\partial y^2} - (c_0 y - k) \frac{\partial \phi}{\partial y} + \max(0, y) \frac{\partial \phi}{\partial z}, & \text{if } z = -1. \end{cases}$$

In the obstacle problem, (this is formal) the generator of  $(X_t, Y_t)$  is defined on any function  $\phi \in C^*(\bar{D})$  such that

$$\phi(\pm 1, y) = \phi(\pm 1, -ey) \text{ in } \pm y > 0$$

satisfies

$$\lim_{t \rightarrow 0} \frac{\mathbb{E}\phi(X_t, Y_t) - \phi(x, y)}{t} = \frac{1}{2} \frac{\partial^2 \phi}{\partial y^2} - (c_0 y + kx) \frac{\partial \phi}{\partial y} + y \frac{\partial \phi}{\partial x}, \text{ if } |x| < 1.$$

**Theorem 6** (Non-standard problems for the elasto-plastic problem). *Consider functions  $u \in C^*(D \times [0, T])$ ,  $v \in C^*(D \times [0, T + h])$ ,  $w \in C^*(D \times [0, T])$ . Assume that  $u, v, w$  satisfy  $(\mathcal{A}_\lambda^u), (\mathcal{A}_\mu^v), (\mathcal{A}_{\lambda+\mu}^w)$ , respectively, (w.r.t to the solution of (3))*

$$(13) \quad \frac{\partial u}{\partial t} + Lu - \lambda u = -g \text{ in } D_T, \quad \frac{\partial u}{\partial t} + L_\pm u - \lambda u = -g \text{ in } D_T^\pm, \quad u(T) = f \text{ in } D.$$

$$(14) \quad \frac{\partial v}{\partial t} + Lv - \mu v = -\psi \text{ in } D_{T+h}, \quad \frac{\partial v}{\partial t} + L_\pm v - \mu v = -\psi \text{ in } D_{T+h}^\pm, \quad v(T+h) = \phi \text{ in } D.$$

$$(15) \quad \frac{\partial w}{\partial t} + Lw - (\lambda + \mu)w = -\frac{\partial u}{\partial y} \frac{\partial v}{\partial y} \text{ in } D_T, \quad \frac{\partial w}{\partial t} + L_\pm w - (\lambda + \mu)w = -\frac{\partial u}{\partial y} \frac{\partial v}{\partial y} \text{ in } D_T^\pm, \quad w(T) = 0 \text{ in } D$$

then the corresponding  $A$  and  $A'$  satisfy

$$A = u(x, y, 0) \quad \text{and} \quad A' = (uv + w)(x, y, 0).$$

**Theorem 7** (Non-standard problems for the obstacle problem). *Consider functions  $u \in C^*(D \times [0, T])$ ,  $v \in C^*(D \times [0, T + h])$ ,  $w \in C^*(D \times [0, T])$ . Assume that  $u, v, w$  satisfy  $(\mathcal{A}_\lambda^u), (\mathcal{A}_\mu^v), (\mathcal{A}_{\lambda+\mu}^w)$ , respectively, (w.r.t to the solution of (5))*

$$(16) \quad \frac{\partial u}{\partial t} + Lu - \lambda u = -g \text{ in } D_T, \quad u(\pm 1, y) = u(\pm 1, -ey) \text{ in } D_T^\pm, \quad u(T) = f \text{ in } D.$$

$$(17) \quad \frac{\partial v}{\partial t} + Lv - \mu v = -\psi \text{ in } D_{T+h}, \quad v(\pm 1, y) = v(\pm 1, -ey) \text{ in } D_{T+h}^\pm, \quad v(T+h) = \varphi \text{ in } D.$$

$$(18) \quad \frac{\partial w}{\partial t} + Lw - (\lambda + \mu)w = -\frac{\partial u}{\partial y} \frac{\partial v}{\partial y} \text{ in } D_T, \quad w(\pm 1, y) = w(\pm 1, -ey) \text{ in } D_T^\pm, \quad w(T) = 0 \text{ in } D$$

then the corresponding  $A$  and  $A'$  satisfy

$$A = u(x, y, 0) \quad \text{and} \quad A' = (uv + w)(x, y, 0).$$

### 3. NUMERICAL COMPUTATION OF $A, B, C$ AND $A', B', C'$

In this section, we first explain the probabilistic numerical approach for SVIs of the elasto-plastic (3) and obstacle (5) problems. Then, we present a numerical approach for solving non-standard BKEs. The method is first presented and applied to the elasto-plastic problem (13), (14) and (15). Then, it is applied to the obstacle problem, (16), (17) and (18).

**3.1. Discretization of SVIs and Monte Carlo approach.** For the probabilistic numerical scheme of  $\{(Z_t, Y_t), t \geq 0\}$  of (3), we use a time step  $\delta t > 0$ . Then we construct random variables  $\{(Z_n, Y_n), 1 \leq n \leq N_{\delta t}\}$  and a partition of  $[0, T]$ ,  $0 = t_0 < t_1 < t_2 < \dots < t_{N_{\delta t}} = T$ . Here, for each  $1 \leq n \leq N_{\delta t}$ ,  $(Z_n, Y_n)$  is an approximation of  $(Z_{t_n}, Y_{t_n})$ . We refer to [3] for a detailed presentation of the algorithm. To be concise, we only explain the computation of quantities of type  $A$ . For any choice of well-behaved functions  $f$  and  $g$ , we proceed with the following approximation

$$(19) \quad \mathbb{E} \left( f(Z_T, Y_T) + \int_0^T g(Z_\tau, Y_\tau) d\tau \right) \approx \frac{1}{M} \sum_{m=1}^M \left( f(Z_{N_{\delta t}}^m, Y_{N_{\delta t}}^m) + \sum_{n=0}^{N_{\delta t}-1} g(Z_n^m, Y_n^m)(t_{n+1} - t_n) \right)$$

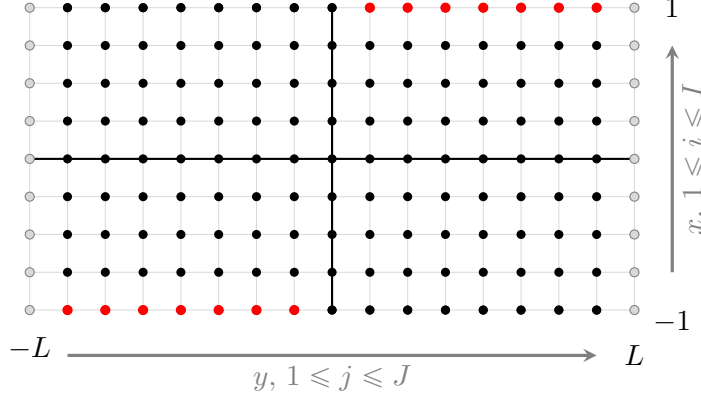


FIGURE 1. Discretization of  $D$ . At black points, the discretized equation is satisfied. At grey points, homogeneous Neumann boundary conditions are used, and at red points non-standard boundary conditions are employed.

where  $\{(Z^m, Y^m), m = 1, \dots, M\}$  is an i.i.d. sequence of trajectories produced by the algorithm.

Details of the probabilistic numerical scheme to compute  $\{(X_t, Y_t), t \geq 0\}$  in (5) are given in Appendix A. Then we use a similar approximation to that given by (19) in terms of  $(X, Y)$  of (5).

**3.2. Discretization of PDE problems.** To numerically approximate the solutions of (13), (14) and (15), we use a finite difference scheme. We truncate the unbounded domain  $D$  to obtain  $D_Y \triangleq (-1, 1) \times (-Y, Y)$ , where  $Y$  is chosen sufficiently large that the probability of finding the underlying process outside  $D_Y$  is negligible. We apply a homogeneous Neumann boundary condition at  $y = \pm Y$ . We consider a two-dimensional rectangular finite difference grid,

$$\mathcal{G} \triangleq \{(z_i, y_j) \triangleq (-1 + (i-1)\delta z, -Y + (j-1)\delta y)\}_{1 \leq i \leq I, 1 \leq j \leq J},$$

where  $\delta z \triangleq \frac{2}{I-1}, \delta y \triangleq \frac{2Y}{J-1}$ . Here,  $I, J$  are odd integers of the form  $2\tilde{I} + 1, 2\tilde{J} + 1$ . The total number of nodes in  $\mathcal{G}$  is  $N = IJ$ . The numerical approximations of  $u(z_i, y_j, t_n)$ ,  $v(z_i, y_j, t_n)$  and  $w(z_i, y_j, t_n)$  are denoted by  $u_{i,j}^n$ ,  $v_{i,j}^n$  and  $w_{i,j}^n$  and the corresponding vectors collecting all the unknowns are  $\mathbf{u}^n$ ,  $\mathbf{v}^n$  and  $\mathbf{w}^n$ . We use the notation  $f_{i,j}, g_{i,j}, \psi_{i,j}, \varphi_{i,j}$  for  $f(x_i, y_j), g(x_i, y_j), \psi(x_i, y_j)$  and  $\varphi(x_i, y_j)$  and the corresponding vectors are  $\mathbf{f}, \mathbf{g}, \boldsymbol{\varphi}, \boldsymbol{\psi}$ . Here,  $t_n \triangleq n\delta t$  discretizes the time and  $N_T\delta t = T$ ,  $N_{T+h}\delta t = T+h$ . Using an implicit Euler method to discretize in time together with finite differences in space, the first conditions in (13), (14) and (15) at the black points in Figure 1 result in

$$\left\{ \begin{array}{l} u_{i,j}^0 = f_{i,j} \quad \text{and} \quad \frac{u_{i,j}^{n+1} - u_{i,j}^n}{\delta t} - (L\mathbf{u}^{n+1})_{i,j} + \lambda u_{i,j}^{n+1} = g_{i,j}, \quad 1 \leq n \leq N_T - 1, \\ v_{i,j}^0 = \varphi_{i,j} \quad \text{and} \quad \frac{v_{i,j}^{n+1} - v_{i,j}^n}{\delta t} - (L\mathbf{v}^{n+1})_{i,j} + \mu v_{i,j}^{n+1} = \psi_{i,j}, \quad 1 \leq n \leq N_{T+h} - 1, \\ w_{i,j}^0 = 0 \quad \text{and} \quad \frac{w_{i,j}^{n+1} - w_{i,j}^n}{\delta t} - (L\mathbf{w}^{n+1})_{i,j} = (D_y\mathbf{u}^n)_{i,j} (D_y\mathbf{v}^n)_{i,j}, \quad 1 \leq n \leq N_T - 1, \end{array} \right.$$

where  $(D_y \mathbf{u})_{i,j}$  and  $(L\mathbf{u})_{i,j}$  are centered finite differences,

$$(D_y \mathbf{u})_{i,j} \triangleq \frac{u_{i,j+1} - u_{i,j-1}}{2\delta y}$$

and first order upwind differences

$$(20) \quad -(L\mathbf{u})_{i,j} \triangleq -(L_y \mathbf{u})_{i,j} - \max(0, y_j) \left( \frac{u_{i+1,j} - u_{i,j}}{\delta z} \right) - \min(0, y_j) \left( \frac{u_{i,j} - u_{i-1,j}}{\delta z} \right)$$

with

$$-(L_y \mathbf{u})_{i,j} \triangleq -\frac{1}{2} \left( \frac{u_{i,j+1} - 2u_{i,j} + u_{i,j-1}}{\delta y^2} \right) - \max(0, b_{i,j}) \left( \frac{u_{i,j+1} - u_{i,j}}{\delta y} \right) - \min(0, b_{i,j}) \left( \frac{u_{i,j} - u_{i,j-1}}{\delta y} \right).$$

The nonstandard boundary conditions (second condition) in (13), (14) and (15) at the red points in Figure 1 are discretized by the same formulae with  $L$  replaced by  $L_{\pm}$ . Here,  $(L_{\pm} \mathbf{u})_{i,j}$  are defined by

$$(21) \quad -(L_+ \mathbf{u})_{i,j} \triangleq -(L_y \mathbf{u})_{i,j} - \min(0, y_j) \left( \frac{u_{i,j} - u_{i-1,j}}{\delta z} \right)$$

and

$$(22) \quad -(L_- \mathbf{u})_{i,j} \triangleq -(L_y \mathbf{u})_{i,j} - \max(0, y_j) \left( \frac{u_{i+1,j} - u_{i,j}}{\delta z} \right).$$

The Neumann boundary conditions at the points shown in grey results in

$$(23) \quad (N_2 \mathbf{u})_{i,j} = 0, \quad (N_2 \mathbf{v})_{i,j} = 0, \quad (N_2 \mathbf{w})_{i,j} = 0, \quad \text{where} \quad (N_2 \mathbf{u})_{i,j} \triangleq \begin{cases} \frac{u_{i,j+1} - u_{i,j}}{\delta y} & \text{if } j = 1, \\ \frac{u_{i,j} - u_{i,j-1}}{\delta y} & \text{if } j = J. \end{cases}$$

This results in the following linear system to be solved in each time step:

$$(24) \quad (I + \delta t M) \mathbf{u}^{n+1} = \mathbf{u}^n + \delta t \mathbf{g}, \quad \mathbf{u}^0 = \mathbf{f},$$

where  $M$  is a sparse  $N \times N$ -matrix that does not depend on  $n$ .

For the computational results presented in the remainder of this paper, we use a C code that implements a Monte Carlo (MC) probabilistic simulation to approximate the solution of (3). We use a MATLAB implementation for the PDE approach (24). Here, an LU factorization is used for solving the linear systems arising from the PDE-approach. For time-dependent PDE simulations, the LU factors are computed once upfront and reused throughout the simulation. Implementations are available upon request.

**3.3. Numerical results for the elasto-plastic problem.** We first present an empirical study on the convergence of the probability of the plastic state ( $E_1$ ) and the mean kinetic energy ( $E_2$ ). The results presented in Figure 2 provide insight into the dependence of the PDE solution on the domain truncation  $L$  and on the number of discretization points. Note in particular, that the convergence of  $\mathbb{E}(Y_T^2)$  requires a sufficiently large value of  $L$ , which is due to the fact that this quantity involves squared  $y$ -values. Moreover, we also observe that

a sufficiently fine mesh with  $\tilde{I} = \tilde{J} \geq 100$  is required to properly resolve the PDE problem.

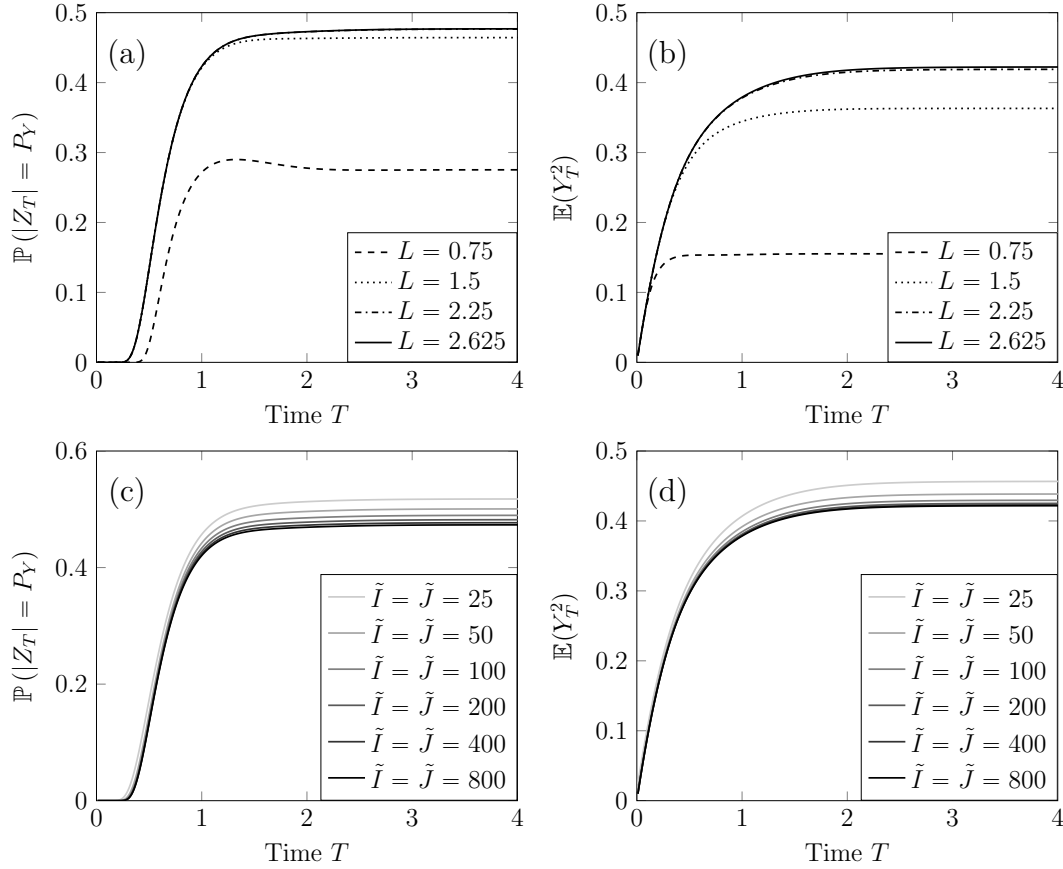


FIGURE 2. Empirical convergence study for  $\mathbb{P}(|Z_T| = P_Y)$  and  $\mathbb{E}(Y_T^2)$ ,  $T \in [0, 4]$ . In all cases,  $c_0 = 1, k = 1, P_Y = 0.25$ . PDE solutions of the probability of plastic state and the mean kinetic energy are shown for different values of the truncation bound  $L$  (while  $\delta y = 0.0075$  is kept constant) in the  $y$ -direction in (a) and (b), and different values of  $\tilde{I} = \tilde{J}$  in (c) and (d) while keeping  $L = 3.0$ .

Next, in Figure 3, we present systematic numerical comparisons between the PDE and the probabilistic Monte Carlo (MC) approach. In particular, we show comparisons for the quantities  $(E_1)$ ,  $(E_2)$ ,  $(E_3)$ , and  $(E_4)$ . We have chosen discretization parameters, for which we found small approximation errors in our previous tests summarized in Figure 2. As can be seen, the results found from the PDE solution closely track the results from the probabilistic simulation. However, some quantities are harder to approximate than others and it appears that for the correlation structure in the kinetic energy, as shown in Figure 3(d), there is a slight discrepancy between the PDE and probabilistic results. This may be related to the fact that the quantity is quartic in the velocity. From Figure 3, we observe as expected from theory (see [8]) that  $(Z_T, Y_T)$  has a unique invariant probability measure. Thus, when  $T$  becomes large, for any well-behaved function  $f$ ,  $\mathbb{E}f(Z_T, Y_T)$  becomes constant

and  $\mathbb{E} \left( \int_0^T f(Z_t, Y_t) dt \right)^2$  obeys linear growth with respect to  $T$ . To the best of our knowledge, except quantities of type  $A$  for large time [3, 10], quantities of type  $A, B, C$  or  $A', B', C'$  (both transient and stationary case) have not been computed using PDE formulations in such a general framework previously.

**3.4. Numerical results for the obstacle problem.** Next, we present numerical results for the stochastic obstacle problem. As above, for the PDE formulation (16), (17) and (18) we use a finite-difference scheme in space and the implicit Euler method in time. The main difference compared to the discretization for the elasto-plastic problem presented in Section 3.2 is in the discretization of the non-standard boundary conditions to be satisfied at the red points in Figure 1. We recall that the boundary conditions on  $D_T^\pm$  in the PDEs for the elasto-plastic and obstacle problems are different because they reflect different boundary behaviors for the underlying stochastic processes. In the elasto-plastic problem, the boundary condition (plastic phases) solves a boundary value problem whose boundary data is also a part of the problem. In the obstacle problem, the boundary condition (impacts with the obstacle) consists in identifying the values of the solution on  $D_T^\pm$  to those on  $x = \pm 1, \mp y > 0$ .

$$\begin{aligned} u_{1,j} &= c_j u_{1,j_e} + (1 - c_j) u_{1,j_e+1} \quad \text{and} \quad v_{1,j} = c_j v_{1,j_e} + (1 - c_j) v_{1,j_e+1} \quad \text{for } 1 \leq j \leq \tilde{J}, \\ u_{I,j} &= c_j u_{I,j_e} + (1 - c_j) u_{I,j_e+1} \quad \text{and} \quad v_{I,j} = c_j v_{I,j_e} + (1 - c_j) v_{I,j_e+1} \quad \text{for } \tilde{J} + 2 \leq j \leq J, \end{aligned}$$

where

$$j_e \triangleq 1 + \left\lceil \frac{1}{\delta y} (L_y - e y_j) \right\rceil \quad \text{and} \quad c_j \triangleq \frac{y_{j_e+1} + e y_j}{\delta y}.$$

We note that  $y_j$  is defined to be on the grid, but, in general, the quantity  $e y_j$  will not correspond to a grid point for  $e \in (0, 1)$ . Consequently, the value imposed in  $u_{1,j}$  (or in  $u_{I,j}$ ) is a value interpolated between the values of  $u$  at the two nearest neighbors of  $-e y_j$  in the grid. Here we use the notation  $[a]$  for the integer part of  $a$ . In the purely elastic case  $e = 1$ ,  $j_1 = J - (j - 1)$  and  $c_j = 1$  whereas in the purely inelastic case  $e = 0$ ,  $j_0 \equiv \tilde{J} + 1$  and  $c_j = 1$ .

In Figure 4, we present numerical comparisons between the PDE and probabilistic MC approaches for  $(E'_2)$  and  $(E'_3)$ . As can be seen, the solution of the PDE approach agrees well with the solution of the probabilistic simulation. We also observe that when  $T$  becomes large, the expectation (left plot) becomes constant and the variance (right plot) grows linearly. While we expect that ergodicity holds for the obstacle problem, to the best of our knowledge this has not been proven in the literature. Additionally, as far as we are aware of, quantities of type  $A, B, C$  or  $A', B', C'$  (both transient and stationary case) have not been computed using PDEs in such a general framework before. Observe that  $(E'_2)$  and  $(E'_3)$  are of type  $A$  and  $A'$  when  $T$  is finite.

**3.5. Long-time behavior.** Next, we present results for the solution of the stationary versions of (13) combined with (15), and of (16) combined with (18) where  $\lambda$  is chosen small enough. We remind the reader that  $\lambda u$  approximates a quantity of the form  $\lim_{t \rightarrow \infty} \mathbb{E} f(Z_t, Y_t)$  when  $\lambda$  is small. We use a similar finite-difference procedure as above for the time-dependent case to obtain a linear system of the form

$$(25) \quad (\lambda I + M) \mathbf{u} = \mathbf{f}.$$

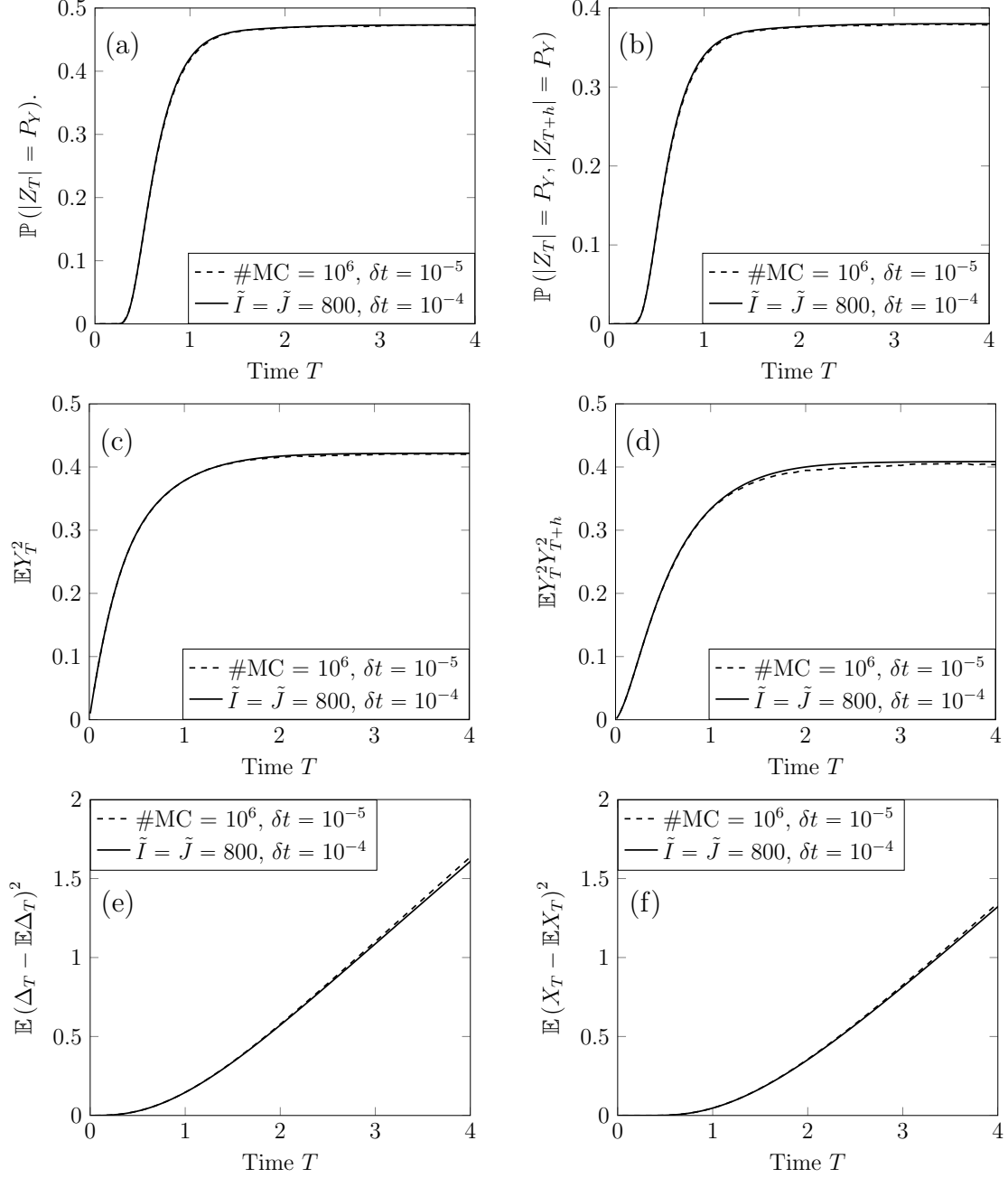


FIGURE 3. Comparison between the PDE (solid) and MC (dashed) solutions for  $T \in [0, 4]$  for the elasto-plastic problem. (a): probability of the plastic state  $\mathbb{P}(|Z_T| = P_Y)$ . (b): a correlation structure of the probability of the plastic state  $\mathbb{P}(|Z_T| = P_Y, |Z_{T+h}| = P_Y)$ ,  $h = 0.2$ . (c): mean kinetic energy  $\mathbb{E}Y_T^2$ . (d): a correlation structure of the mean kinetic energy  $\mathbb{E}Y_T^2 Y_{T+h}^2$ . (e): the variance of the plastic deformation  $\mathbb{E}(\Delta_T - \mathbb{E}\Delta_T)^2$ . (f): the variance of the total deformation  $\mathbb{E}(X_T - \mathbb{E}X_T)^2$ .

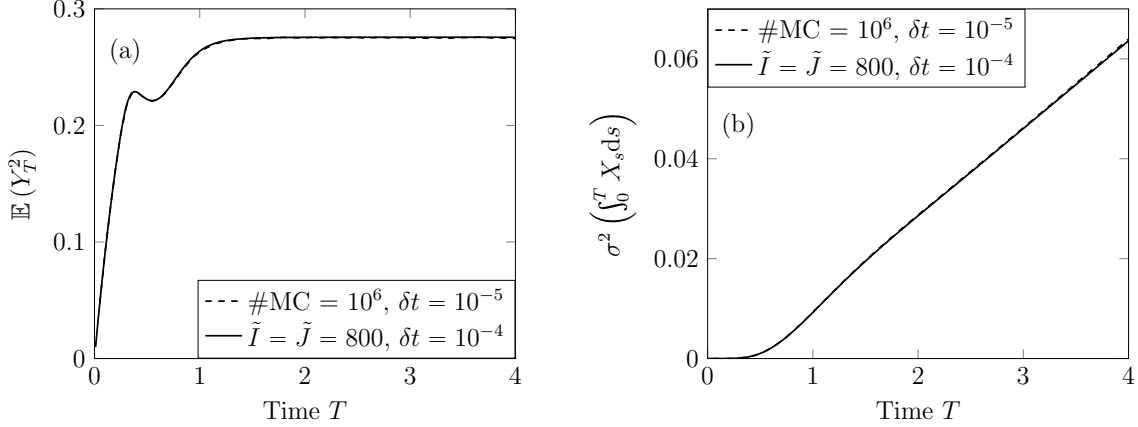


FIGURE 4. Obstacle problem with  $e = 0.5$ . Comparison between the PDE (solid) and MC (dashed) solutions for  $T \in [0, 4]$ . (a): mean kinetic energy  $\mathbb{E}(Y_T^2)$ . (b): the variance of the integral of the total deformation  $\sigma^2\left(\int_0^T X_s ds\right)$ .

Again, we first compare results computed using the discretized PDE approach (25) with results based on Monte Carlo simulations. For the elasto-plastic PDE discretization, we use  $\tilde{I} = \tilde{J} = 800$ , i.e., the overall number of spatial unknowns is  $(2\tilde{I} + 1)(2\tilde{J} + 1) = 2,563,201$ , and we choose  $\lambda = 10^{-3}$ . For the Monte Carlo simulation, we use  $\delta t = 10^{-5}$ . We present the comparison between the PDE and the Monte Carlo (MC) approach in Table 2. For the obstacle problem, the spatial discretization uses  $\tilde{I} = \tilde{J} = 500$ , amounting to overall 1,002,001 unknowns. We again use  $\lambda = 10^{-3}$ . Results of the comparison between the PDE and the Monte Carlo approach are given in Table 3. As can be seen, for both the obstacle as well as the elasto-plastic problem, the results obtained with Monte Carlo are close to the PDE results. To study the interplay between the time discretization and the Monte Carlo errors, we considered the case of the growth rate of the variance related to the plastic deformation in the elasto-plastic problem. Approximations of  $(E_1)$  and  $(E_3)$  are shown in Table 1 for  $P_Y = 0.25$  and for different values of  $\delta t$  and  $T$ . The approximation of  $(E_1)$  is given by (19) with  $g = 0$  and  $f(y, z) = \mathbf{1}_{\{|z|=P_Y\}}$  and the approximation of  $(E_3)$  is given by

$$\frac{1}{TM} \sum_{m=1}^M \left( \sum_{n=0}^{N_{\delta t}-1} g(Z_n^m, Y_n^m)(t_{n+1} - t_n) \right)^2,$$

where  $g(y, z) = y \mathbf{1}_{\{|z|=1\}}$ . In both approximations,  $(Z_n^m, Y_n^m)$  satisfies the probabilistic numerical scheme for (3) and the Monte Carlo sample size is  $10^5$ . For the approximation of  $(E_1)$  we observe a relatively fast convergence towards a constant with respect to  $T \geq 3$  whereas for the approximation of  $(E_3)$  a sufficiently large value of  $T \geq 150$  is required to see the convergence. For both cases, a sufficiently small value of  $\delta t = 10^{-4}$  is required. Empirically, the data indicates that the error is roughly halved as the time step is divided by 10.

#### 4. COMPARISON WITH [3, 6, 10] FOR A WHITE NOISE EPPO AT LARGE TIME

In this section, we compare the approach proposed here with previous techniques employed for a white noise EPPO.

TABLE 1. Results using the MC approach with different  $T$  and  $\delta t$  for the approximation of the probability ( $E_1$ ) (left) and the growth rate of the plastic deformation ( $E_3$ ) (right). Here  $P_Y = 0.25$ .

$T$	$\delta t = 10^{-2}$	$\delta t = 10^{-3}$	$\delta t = 10^{-4}$	$T$	$\delta t = 10^{-2}$	$\delta t = 10^{-3}$	$\delta t = 10^{-4}$
2	0.518	0.487	0.474	10	0.489	0.464	0.456
4	0.519	0.492	0.478	20	0.532	0.505	0.493
8	0.519	0.489	0.477	40	0.558	0.528	0.510
16	0.520	0.487	0.481	80	0.567	0.538	0.521
32	0.518	0.491	0.478	160	0.575	0.548	0.524
64	0.519	0.490	0.476	200	0.574	0.547	0.526

TABLE 2. Results using PDE and MC method approaches for the elasto-plastic problem (3) for different plastic yields  $P_Y$ : Probability ( $E_1$ ) of plastic state for  $T \rightarrow \infty, (T \geq 5)$ . Asymptotic growth rate ( $E_3$ ) of the plastic/total deformation for  $T \rightarrow \infty, (T \geq 150)$ .

	$P_Y$	0.1	0.2	0.3	0.4	0.5	0.6	0.7	0.8	0.9	1.0
$(E_1)$	<b>PDE</b>	0.638	0.521	0.430	0.354	0.289	0.234	0.187	0.148	0.115	0.088
$T \rightarrow \infty$	<b>MC</b>	0.639	0.521	0.429	0.352	0.286	0.230	0.184	0.144	0.112	0.085
$(E_3)$	<b>PDE</b>	0.776	0.589	0.440	0.325	0.238	0.173	0.125	0.089	0.064	0.045
$T \rightarrow \infty$	<b>MC</b>	0.799	0.607	0.457	0.337	0.248	0.182	0.132	0.096	0.070	0.050

TABLE 3. Results using PDE and MC method approaches for the obstacle problem (5) for different position of the obstacle  $P_O$ : Mean kinetic energy ( $E'_2$ ) for  $T \rightarrow \infty, (T \geq 5)$ . Asymptotic growth rate ( $E_3$ ) of the integral of the deformation for  $T \rightarrow \infty, (T \geq 150)$ .

	$P_Y$	0.1	0.2	0.3	0.4	0.5	0.6	0.7	0.8	0.9	1.0
$(E'_2)$	<b>PDE</b>	0.179	0.250	0.298	0.347	0.364	0.388	0.409	0.426	0.441	0.453
$T \rightarrow \infty$	<b>MC</b>	0.179	0.250	0.297	0.334	0.364	0.389	0.408	0.423	0.437	0.450
$(E_3)$	<b>PDE</b>	0.00148	0.0097	0.028	0.062	0.103	0.158	0.223	0.294	0.370	0.447
$T \rightarrow \infty$	<b>MC</b>	0.00149	0.0097	0.028	0.060	0.103	0.158	0.222	0.295	0.370	0.447

4.1. **Approach in [3] for the elasto-plastic Poisson problem.** If the values of the function  $u$  were known at  $z = P_Y, y = 0^+$  and  $z = -P_Y, y = 0^-$ , the stationary version of (13) would be a degenerate elliptic PDE with a standard Dirichlet boundary condition. This PDE could be solved by a standard numerical approach. However, the challenge in solving this problem resides in the fact that these values are not input data of the problem but part of the solution. This makes it a non-standard problem and more challenging to solve. As a remedy, a superposition approach has been proposed in [3]. To ensure continuity of  $u$  at the points  $(P_Y, 0)$  and  $(-P_Y, 0)$ , the linearity of (13) allows to compute the solution as a linear combination of the following three local problems:

$$\lambda v + A_2 v = g \text{ in } D_2, \quad \lambda v + B_{2,+} v = g_+ \text{ in } D_2^+, \quad \lambda v + B_{2,-} v = g_- \text{ in } D_2^-,$$

$$\text{with } v(P_Y, 0) = 0, v(-P_Y, 0) = 0,$$

$$\lambda\pi^+ + A_2\pi^+ = 0 \text{ in } D_2, \quad \lambda\pi^+ + B_{2,+}\pi^+ = 0 \text{ in } D_2^+, \quad \lambda\pi^+ + B_{2,-}\pi^+ = 0 \text{ in } D_2^-,$$

$$\text{with } \pi^+(P_Y, 0) = 1, \pi^+(-P_Y, 0) = 0,$$

$$\lambda\pi^- + A_2\pi^- = 0 \text{ in } D_2, \quad \lambda\pi^- + B_{2,+}\pi^- = 0 \text{ in } D_2^+, \quad \lambda\pi^- + B_{2,-}\pi^- = 0 \text{ in } D_2^-,$$

$$\text{with } \pi^-(P_Y, 0) = 0, \pi^-(-P_Y, 0) = 1.$$

Then, finding a continuous solution  $u$  amounts to finding scalar values  $u_+$  and  $u_-$  such that  $u = v + u_+\pi^+ + u_-\pi^-$  is continuous in  $(-P_Y, 0)$  and  $(P_Y, 0)$ , which requires to solve the following linear  $2 \times 2$  system:

$$\Pi \begin{pmatrix} u_+ \\ u_- \end{pmatrix} = \begin{pmatrix} v(P_Y, 0^-) - v(P_Y, 0^+) \\ v(-P_Y, 0^-) - v(-P_Y, 0^+) \end{pmatrix},$$

where

$$\Pi \triangleq \begin{pmatrix} \pi^+(P_Y, 0^+) - \pi^+(P_Y, 0^-) & \pi^-(P_Y, 0^+) - \pi^-(P_Y, 0^-) \\ \pi^+(-P_Y, 0^+) - \pi^+(-P_Y, 0^-) & \pi^-(-P_Y, 0^+) - \pi^-(-P_Y, 0^-) \end{pmatrix}.$$

**Remark 8.** *It is important to note that this technique in [3] is based on the superposition of local PDEs and is thus specific to the case of a SVI modelling an elasto-perfectly-plastic oscillator (EPPO) excited by white noise. It has no natural extension to more general EP or obstacle problems. Indeed, as explained above, solving the KE with non-standard boundary conditions corresponding to an EPPO excited by white noise reduces to solving two linear equations for two unknown scalars. For more general problems as targeted here, one must find unknown functions, and thus the superposition method cannot be employed straightforwardly. This superposition technique has a probabilistic interpretation in terms of novel notion of short cycles as defined in [5].*

#### 4.2. Approach in [6, 10] for the growth rate of the variance of $\Delta_t$ at large time.

In [6], the growth rate of the variance of  $\Delta_t$  at large time has been characterized. Relying on (3), the authors proposed a novel and simple formulation of the evolution of the system in terms of stopping times in order to identify a repeating pattern in the trajectory, namely long cycles. This concept is summarized next.

**Definition 9.** *A long cycle of the solution  $(Z_t, Y_t)$  of (3) is a path, enclosed by the stopping times  $\tau_0$  and  $\tau_1$  defined below, starting and ending in one of the two points  $\{(-P_Y, 0), (P_Y, 0)\}$  which has touched the other point at least once. Similarly, a half long cycle is a path enclosed by the stopping times  $\tau_0$  and  $s_0$ , or by  $s_0$  and  $\tau_1$ . In a recursive way, a sequence of stopping times  $\tau_n$  can be defined where  $\tau_n$  is the time when the  $n$ -th long cycle ends.*

With the notation

$$\tau_0 \triangleq \inf\{t > 0, \quad Y_t = 0 \quad \text{and} \quad |Z_t| = P_Y\},$$

$\delta \triangleq \text{sign}(Z_{\tau_0})$ , which labels the first boundary reached by the process  $(Z_t, Y_t)$ , and

$$\begin{cases} s_0 \triangleq \inf\{t > \tau_0, \quad Y_t = 0 \quad \text{and} \quad Z_t = -\delta P_Y\}, \\ \tau_1 \triangleq \inf\{t > s_0, \quad Y_t = 0 \quad \text{and} \quad Z_t = \delta P_Y\}, \end{cases}$$

they obtained a probabilistic expression for the coefficient of the growth rate of the variance of  $\Delta_t$  as follows:

$$(26) \quad \lim_{t \rightarrow \infty} \frac{\sigma^2(\Delta_t)}{t} = \mu \gamma^2,$$

where

$$(27) \quad \gamma^2 \triangleq \mathbb{E}(\Delta_{\tau_1} - \Delta_{\tau_0})^2 \quad \text{and} \quad \mu \triangleq \frac{1}{\mathbb{E}(\tau_1 - \tau_0)}.$$

In [10], using a Fourier transform approach, an analytic framework for  $\mu$  and  $\gamma^2$  has been proposed.

**Remark 10.** *It is important to note that the technique in [6, 10] of splitting the trajectory in terms of long cycle (an identically independent distributed repeating pattern) is specific to the case of a SVI modelling an EPPO excited by white noise. It has no natural extension to more general EP, obstacle or colored noise problems. Moreover, it cannot be employed for short durations.*

## 5. CONCLUSIONS AND PERSPECTIVES

BKEs with non-standard boundary conditions that describe non-smooth stochastic processes have been (formally) derived and numerically solved. Important examples from engineering have been successfully treated. The present work will pave the way for promising new research. Indeed, the technique presented in this paper is straightforwardly generalizable to a broad range of cases where  $F$  and  $G$  are time-dependent and to problems driven by colored noise. This framework can also be extended to a PDE interpretation of Power Spectral Densities. It can also be employed to solve Hamilton-Jacobi-Bellman Equations and Free Boundary value problems related to the stochastic optimal control and optimal stopping of a class of non-smooth stochastic dynamical systems.

## APPENDIX A. PROBABILISTIC SIMULATION

Below a detailed implementation of the probabilistic simulation for (5). For  $T > 0, N \in \mathbb{N}$  and  $\delta t \triangleq \frac{T}{N}$ . We set  $\Sigma \in \mathbb{R}^{2 \times 2}$  such that

$$(28) \quad \Sigma \Sigma^T = \begin{pmatrix} \sigma_x^2(\delta t) & \sigma_{x,y}(\delta t) \\ \sigma_{x,y}(\delta t) & \sigma_y^2(\delta t) \end{pmatrix}.$$

where

$$\begin{aligned} \sigma_x^2(t) &= \frac{1}{\omega^2} \int_0^t e^{-c_0 s} \sin^2(\omega s) ds, \\ \sigma_y^2(t) &= \int_0^t e^{-c_0 s} \cos^2(\omega s) ds - \frac{4c_0^2}{\omega^2} \int_0^t e^{-c_0 s} \sin^2(\omega s) ds - \frac{c_0}{2\omega^2} e^{-c_0 t} \sin^2(\omega t), \\ \sigma_{xy}(t) &= \frac{1}{2\omega} \int_0^t e^{-c_0 s} \sin(2\omega s) ds - \frac{c_0}{4\omega^2} \int_0^t e^{-c_0 s} \sin^2(\omega s) ds. \end{aligned}$$

Here,  $\omega \triangleq \frac{\sqrt{4k - c_0^2}}{2}$ , it is assumed that  $4k > c_0^2$ . For every  $(x, y) \in \mathbb{R}^2$ , we define

$$M(\delta t, x, y) \triangleq \begin{pmatrix} m_1(\delta t, x, y) \\ m_2(\delta t, x, y) \end{pmatrix}$$

where

$$\begin{aligned} m_1(t, x, y) &= e^{-\frac{c_0 t}{2}} \{x \cos(\omega t) + \frac{1}{\omega} (y + \frac{c_0}{2} x) \sin(\omega t)\}, \\ m_2(t, x, y) &= -\frac{c_0}{2} e_x(t, x, y) + e^{-\frac{c_0 t}{2}} \{-\omega x \sin(\omega t) + (y + \frac{c_0}{2} x) \cos(\omega t)\}. \end{aligned}$$

We can now detail the probabilistic simulation for (5), where the main challenge is the incorporation of the obstacles in the simulation. Let  $(G_{n,m})_{n=0..N, m=1,2}$  be random independent Gaussian  $\mathcal{N}(0, 1)$  variables. To compute the  $(n+1)$ th time step, we attempt to perform the explicit step

$$(29) \quad \begin{pmatrix} X_{n+1} \\ Y_{n+1} \end{pmatrix} \triangleq M\left(\delta t, \begin{pmatrix} X_n \\ Y_n \end{pmatrix}\right) + \Sigma \begin{pmatrix} G_{1,n} \\ G_{2,n} \end{pmatrix}.$$

If we find that the  $(n+1)$ st point does not satisfy the obstacle conditions, for instance since  $X_{n+1} > 1$ , we adjust the step length to  $\theta_{n+1}\delta t$ , with  $\theta_{n+1} \triangleq (1 - X_n)/(X_{n+1} - X_n)$ , and set

$$t_{n+1} \triangleq t_n + \theta_{n+1}\delta t, \quad X_{n+1} \triangleq 1, \quad Y_{n+1} \triangleq -e((1 - \theta_{n+1})Y_n + \theta_{n+1}Y_{n+1}).$$

An analogous reduction of the step length is used if the full step computed in (29) satisfies  $X_{n+1} < -1$ .

#### ACKNOWLEDGEMENT

LM expresses his sincere gratitude to the Courant Institute for being supported as Courant Instructor in 2014 and 2015, when this work was initiated. LM is also supported by a faculty discretionary fund from NYU Shanghai and the National Natural Science Foundation of China, Research Fund for International Young Scientists under the project #1161101053 entitled ‘‘Computational methods for non-smooth dynamical systems excited by random forces’’ and the Young Scientist Program under the project #11601335 entitled ‘‘Stochastic Control Method in Probabilistic Engineering Mechanics’’. LM also thanks the Department of Mathematics of the City University of Hong Kong for the hospitality. JW acknowledges support from the SAR Hong Kong grant [CityU 11306115] ‘‘Dynamics of Noise-Driven Inelastic Particle Systems’’.

#### REFERENCES

- [1] V.I. Babitsky, Theory of vibro-impacts systems and applications, Springer, 1998.
- [2] V. Barbu, G. Daprato The stochastic obstacle problem for the harmonic oscillator with damping, Journal of Functional Analysis 235 (2006) 430-448.
- [3] A. Bensoussan, L. Mertz, O. Pironneau, J. Turi, An Ultra Weak Finite Element Method as an Alternative to a Monte Carlo Method for an Elasto-Plastic Problem with Noise, SIAM J. Numer. Anal. , **47(5)** (2009), 3374–3396.
- [4] A. Bensoussan, L. Mertz, Degenerate Dirichlet problems related to elasto-plastic oscillator excited by a filtered noise, IMA J. Appl. Math. (2015) 80 (5): 1387-1408.

- [5] A. Bensoussan, L. Mertz, An analytic approach to the ergodic theory of stochastic variational inequalities, C. R. Acad. Sci. Paris Ser. I, **350(7-8)**, (2012), 365-370.
- [6] A. Bensoussan, L. Mertz, S.C.P. Yam, Long cycle behavior of the plastic deformation of an elasto-perfectly-plastic oscillator with noise, C. R. Acad. Sci. Paris Sr. I Math. **350(17-18)** (2012), 853-859.
- [7] A. Bensoussan, L. Mertz, S.C.P. Yam, non-standard boundary value problems of a stochastic variational inequality modeling an elasto-plastic oscillator excited by a filtered noise, SIAM J. Math. Anal., (2016)
- [8] A. Bensoussan, J. Turi, Degenerate Dirichlet Problems Related to the Invariant Measure of Elasto-Plastic Oscillators, Applied Mathematics and Optimization, **58(1)** (2008), 1-27.
- [9] A. Bensoussan, J. Turi, On a Class of Partial Differential Equations with non-standard Dirichlet Boundary Conditions, Appl. Num. Par. Diff. Eq. **15**, pp. 9-23 (2010).
- [10] A. Bensoussan, C. Feau, L. Mertz, S.C.P. Yam, An analytical approach for the growth rate of the variance of the deformation related to an elasto-plastic oscillator excited by a white noise, Appl. Math. Res. Express 2015 (1): 99-128.
- [11] M.F. Dimentberg, D.V. Iourtchenko Random vibration with impacts : a review, Nonlinear Dynamics (36): 229-254, 2004.
- [12] C. Feau, Probabilistic response of an elastic perfectly plastic oscillator under Gaussian white noise, Probabilistic Engineering Mechanics, **23(1)** (2008), 36-44.
- [13] P. Glasserman, Monte Carlo Methods in Financial Engineering, Series: Stochastic Modelling and Applied Probability , Vol. 53 2003, XIV, 602 p. 70 illus., Hardcover ISBN: 978-0-387-00451-8.
- [14] M. M. Klosek-Dygas, B. J. Matkowsky, Z. Schuss, Colored noise in dynamical systems, SIAM J. Appl. Math., **48(2)**, 425-441.
- [15] D. Karnopp, T.D. Scharton, Plastic deformation in random vibration, The Journal of the Acoustical Society of America, **39** (1966), 1154-61.
- [16] Rice, S. O, Mathematical analysis of random noise, Bell System Tech. J. 23: 282332.
- [17] P.L. Lions, A.S. Sznitman, Stochastic differential equation with reflecting boundary conditions, Communications on Pure and Applied Mathematics, Vol. XXXVII, 511-537 (1984).
- [18] E. Pardoux, A. Yu. Veretennikov, On the Poisson equation and diffusion approximation : I The Annals of Probability, 2001, Vol. 29, No. 3, 10611085
- [19] G.A. Pavliotis, Stochastic Processes and Applications : Diffusion Processes, the Fokker Planck and Langevin Equation, Texts in Applied Mathematics 60, Springer 2014.
- [20] H. Risken, The Fokker-Planck Equation, Springer Series in Synergetics, Volume 18, 1996.
- [21] D. Talay, Stochastic Hamiltonian Systems, Markov Processes and Related Fields, 8(1-36), 2002.